



Identification of lncRNA Signature of Tumor-Infiltrating T Lymphocytes With Potential Implications for Prognosis and Chemotherapy of Head and Neck Squamous Cell Carcinoma

Liping Wang^{1†}, Gui Yang^{1†}, Guohong Liu^{2*} and Yunbao Pan^{1*}

¹Department of Laboratory Medicine, Zhongnan Hospital of Wuhan University, Wuhan University, Wuhan, China, ²Department of Radiology, Zhongnan Hospital of Wuhan University, Wuhan University, Wuhan, China

OPEN ACCESS

Edited by:

Sharad K. Sharma,
Sanofi U.S., United States

Reviewed by:

Xinmao Song,
Fudan University, China
Wei Cao,
Shanghai Jiao Tong University, China

*Correspondence:

Guohong Liu
lliguoh@outlook.com
Yunbao Pan
panyunbao@outlook.com

[†]These authors have contributed
equally to this work and share first
authorship

Specialty section:

This article was submitted to
Pharmacology of Anti-Cancer Drugs,
a section of the journal
Frontiers in Pharmacology

Received: 14 October 2021

Accepted: 30 December 2021

Published: 15 February 2022

Citation:

Wang L, Yang G, Liu G and Pan Y
(2022) Identification of lncRNA
Signature of Tumor-Infiltrating T
Lymphocytes With Potential
Implications for Prognosis and
Chemotherapy of Head and Neck
Squamous Cell Carcinoma.
Front. Pharmacol. 12:795205.
doi: 10.3389/fphar.2021.795205

Purpose: We systematically analyzed HNSCC-infiltrating T lymphocytes lncRNAs (HILTlncRNAs) to assess their predictive value for the survival outcome and immunotherapy response of patients with anti-programmed death-1 (PD-1) therapy and to evaluate their predictive power to chemotherapeutic agents.

Methods: HNSCC transcriptome and clinical information was obtained from The Cancer Genome Atlas (TCGA) database. Immunocell microarray data were obtained from the Gene Expression Omnibus (GEO) database. T-cell-specific lncRNAs were identified by differential expression analysis. Prognostic paired HILTlncRNAs (PHILTlncRNAs) were filtered and modeled by univariate cox, lasso and multivariate cox regression analysis. To construct lncRNA-miRNA-mRNA competitive endogenous RNA (ceRNA) regulatory networks, differentially expressed mRNAs in HNSCC patients were incorporated, microRNAs and differentially expressed mRNAs interacting with T-cell-specific lncRNAs were filtered out based on miRcode, miRDB, miRTarBase, and TargetScan databases.

Results: 75 T-cell-specific lncRNAs and 9 prognostic PHILTlncRNAs were identified. Low-risk HNSCC patients had a better prognosis and significant immune cell infiltration, driving the immune response. Differential expression of RNA-binding proteins (RBPs), PD-1 and programmed cell death 1 ligand 1 (PD-L1) was demonstrated in the high and low risk groups of HNSCC patients. In the high risk group, high expression of PD-1 improved patient prognosis, whereas the opposite was observed in the low-risk group. The promoter methylation levels of two RBPs (DNMT1 and ZC3H12D) were decreased in HNSCC patients compared with normal samples, their expression levels were positively correlated with PD-1 and PD-L1 levels and T-cell infiltration. Finally, we screened the sensitivity of HNSCC patients to chemotherapeutic agents and found it differed between high and low risk groups.

Conclusion: HILTlncRNAs provided a theoretical basis for immune targeted therapy and drug development.

Keywords: head and neck squamous cell carcinoma, tumor-infiltrating T lymphocytes, long noncoding RNAs, tumor microenvironment, immunotherapy

INTRODUCTION

Head and neck squamous cell carcinoma (HNSCC) occurs mainly in the mucosal epithelium of the pharynx and oral cavity. Although its epidemiology has changed considerably in recent years, with both an incidence decline in cigarette smoking-associated HNSCC and an increase in human papillomavirus (HPV)-associated HNSCC, it remains a heavy burden on healthcare systems worldwide with 930,000 new cases of HNSCC and 470,000 HNSCC-related deaths each year (McDermott and Bowles, 2019; Johnson et al., 2020; Sung et al., 2021).

The tumor microenvironment (TME) consists of various cell types, including tumor cells, immune cells, endothelial cells, adipocytes and fibroblasts, and a variety of structures, such as blood vessels, lymphatic vessels and extracellular matrix, *etc.* The TME plays an important role in tumor growth, invasion, metastasis, diagnosis and treatment. High level of T lymphocyte infiltration in the TME or close to the tumor cell parenchyma may have prognostic value (Lei et al., 2016; Di Martino et al., 2019). High infiltration of CD4⁺ and CD8⁺ T cells in the TME has been associated with improved overall and relapse-free survival in patients with HNSCC, and could serve as an independent prognostic factor (Nguyen et al., 2016). Blockade of the T-cell immunoglobulin mucin 3 (TIM3) receptor reduces immunosuppression by downregulating regulatory T cells (Tregs) in HNSCC (Liu et al., 2018a). Elevated interleukin 23 (IL-23) and IL-6 levels released by HNSCC cells may promote T helper 17 (Th17) cell proliferation (Kesselring et al., 2010), while Th17 and Tregs proliferation is associated with the functional impairment of infiltrating CD8⁺ T cells in HNSCC (Kesselring et al., 2010; Liu et al., 2018b). Restoring exhausted T cells in the TME by blocking TIGIT/CD155 promotes antitumor immunity in HNSCC (Wu et al., 2019).

lncRNAs have been shown to play an important role in HNSCC prognosis. Cao et al. found that KTN1-AS1, LINC00460 and RP5-894A10.6 affected the survival of HNSCC patients (Cao et al., 2017). Wang et al. screened AC02066.1, AC013652.1 and AC016629.3 by cox regression analysis to construct a prognostic model for HNSCC. Three lncRNA co-expressed mRNAs were performed functional enrichment analysis. These mRNAs are involved in the regulation of angiogenesis, cell adhesion and extracellular matrix breakdown (Wang et al., 2018a). Diao et al. identified four lncRNAs including RP11-366H4.1, LINC01123, RP11-110I1.14 and CTD-2506J14.1 which are closely associated with overall survival of HNSCC patients (Diao et al., 2019). Zhang et al. constructed a risk value model for HNSCC based on 15 lncRNAs (FOXO2-AS1, MYOSLID, WFDC21P, AC073130.1, AL078644.1, LINC01234, AC243773.2, C5orf66-AS1, LINC02041, AC012213.4, LINC01305, AC108134.1, ALMS1-IT1, LINC02099 and AC019171.1), which can effectively predict overall survival and stratified patients (Zhang et al., 2019). In particular, lncRNA LINC00460 regulated autophagy of HNSCC cells through regulation of the microRNA (miRNA)-206/stanniocalcin-2 axis (Xue et al., 2019). lncRNA MIR31HG promoted HNSCC cell proliferation by regulating the cell cycle

through HIF1A and p21 (Wang et al., 2018b). lncRNA MX1-215 negatively regulated immunosuppression in HNSCC by interrupting H3K27 acetylation (Ma et al., 2020). An increasing number of studies have reported that immune-related lncRNAs were associated with the diagnosis and prognosis of HNSCC patients (Chen et al., 2021; Yin et al., 2021). However, the function of lncRNAs in the regulation of infiltrating T lymphocytes in HNSCC was not clear, thus we investigated the lncRNA regulatory network of infiltrating T lymphocytes in HNSCC and its clinical significance.

We proposed prognostic paired HNSCC-infiltrating T lymphocytes lncRNAs (PHILTlncRNAs) as new biomarkers for HNSCC, performed a systematic analysis and developed a model of PHILTlncRNAs to guide T lymphocyte infiltration into the HNSCC TME. We also predicted PD-1 immunotherapy response and screened the sensitivity of HNSCC patients to chemotherapy agent. We first extracted T-cell-specific lncRNAs, and then identified paired lncRNAs in HNSCC-infiltrating T lymphocytes (PHILTlncRNAs) to develop models of prognostic, risk assessment, and clinical parameter analysis. Subsequently, we predicted miRNAs and mRNAs which interact with T-cell-specific lncRNAs. Subsequently, we performed functional enrichment analysis and constructed ceRNA networks by intersecting the predicted mRNAs with differentially expressed mRNAs in HNSCC. Based on the developed prognostic model, we performed immune infiltration and immune function gene set enrichment analysis (GSEA), and also investigated the expression, methylation and mutation status of DNMT1, ZC3H12D, PD-1 and PD-L1 in HNSCC, and their effect on T-lymphocyte infiltration. Eventually, drug sensitivity analysis was performed in HNSCC patients to provide a clinical reference for screening of effective drugs.

METHODS

Acquisition of Prognostic PHILTlncRNAs and Model Development

Transcriptomic data and clinical information of HNSCC were downloaded from The Cancer Genome Atlas (TCGA) database. Microarray data for T cells (GSE5105) and other immune cells (GSE59237, GSE6863, GSE23371, GSE25320, GSE27838, GSE28698, GSE37750, GSE39889, GSE8059, GSE49910 and GSE42058) based on the Affymetrix platform were downloaded from the Gene Expression Omnibus (GEO) database. The data were annotated by gene transfer format files obtained from Ensembl (<http://asia.ensembl.org>) and lncRNAs were filtered. The data were corrected using methods of ComBat in sva R package and normalizeBetweenArrays in limma R package. The differential expression analysis of lncRNAs between T cells and other immune cells was performed using limma R package to identify T-cell-specific lncRNAs ($|\log_2FC| > 1$, FDR < 0.05). The intersected lncRNAs of T-cell-specific lncRNAs with lncRNAs in HNSCC were filtered to obtain HILTlncRNAs. These HILTlncRNAs were cyclically paired to construct a 0-or-1 matrix, in which when HILTlncRNA A is expressed at a higher level than HILTlncRNA

B, the value is 1, otherwise it is 0. The pairs of lncRNAs with a value of 0 or 1 were successfully paired when they accounted for 20–80% of the total samples, and these successfully paired PHILTlncRNAs were designated as PHILTlncRNAs. The prognostic candidate PHILTlncRNAs were filtered by univariate Cox regression analysis using the survival R package ($p < 0.01$), further screened by Lasso regression analysis. Those screened PHILTlncRNAs were used to perform multivariate Cox regression analysis to filter out the most prognostic PHILTlncRNAs. These identified PHILTlncRNAs were used to construct risk models using the survival, survminer and glmnet R packages. The risk score formula was as follows: Risk score = PHILTlncRNA1* β (PHILTlncRNA1) + PHILTlncRNA2* β (PHILTlncRNA2) + PHILTlncRNAi* β (PHILTlncRNAi), where β represents the regression coefficient values. The ROC curves were plotted using Kaplan-Meier method in survivalROC R package. The maximum value of sum of specificity and sensitivity was used as the cutoff value. HNSCC patients with risk score greater than the cutoff value are in the high risk group and the opposite in the low risk group.

Assessing the Prognostic Value of PHILTlncRNAs

To assess the effectiveness of PHILTlncRNAs to predict survival, we performed Kaplan-Meier survival analysis using log-rank tests in the survival and survminer R packages between high and low risk groups. We further explored the survival status of HNSCC patients with increasing risk scores. The distribution of clinical parameters including age, gender, grade, stage and TMN stage of HNSCC patients in high and low risk groups were plotted using chi-squared test in the ComplexHeatmap R package. The differential level of risk scores among patients with different gender, or grade, or TN staging were derived using the Wilcoxon test in limma and ggpubr R packages. Finally, we performed univariate and multivariate Cox regression analysis for clinical parameters of age, gender, grade, stage, and risk scores in predicting survival of HNSCC patients using the survival R package, and thus accessed the feasibility of our model.

ceRNA Network of HNSCC-Infiltrating T Lymphocytes

We predicted the interactions between T-cell-specific lncRNAs and miRNAs using the miRcode database (<http://www.mircode.org/>), identified the target mRNAs of miRNAs using the miRDB (<http://mirdb.org/>), miRTarBase (<http://miRTarBase.cuhk.edu.cn/>) and TargetScan (<http://www.targetscan.org>) databases. Hub mRNAs were obtained by intersecting the identified mRNAs with the differentially expressed mRNAs of HNSCC patients ($|\log_{2}FC| > 2$, FDR < 0.05) using the Wilcoxon test. Subsequently, the corresponding lncRNAs and miRNAs which interact with the hub mRNAs were screened using cytoscape software to construct the ceRNA network. To characterize the molecular pathways in which these hub mRNAs are involved, we performed Kyoto Encyclopedia of Genes and Genomes (KEGG) and Gene Ontology (GO)

enrichment analysis. The above procedures were conducted with R packages including limma, org.Hs.eg.db and clusterProfiler.

Analysis of Immune Cell Infiltration

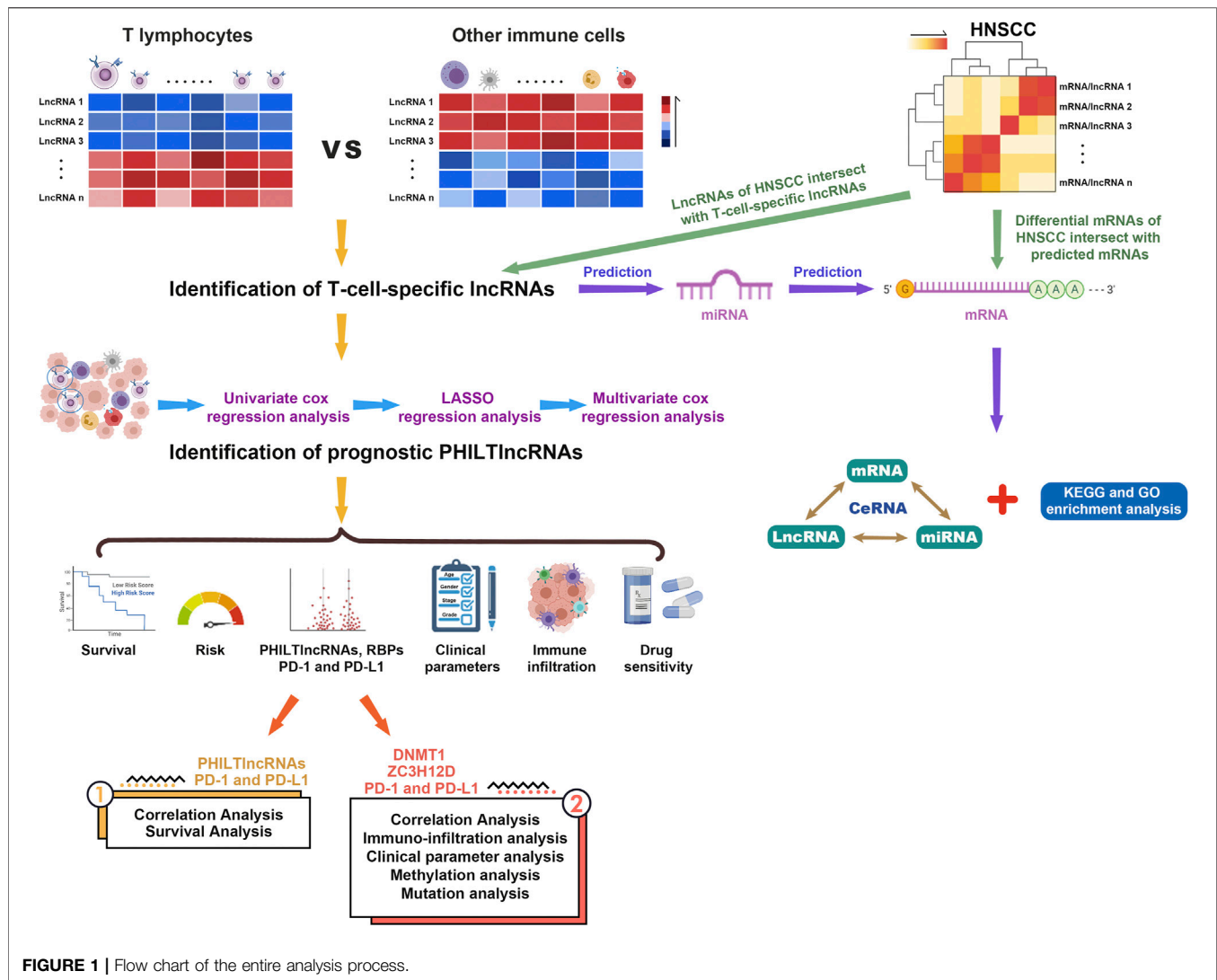
We performed differential analysis of immune cell infiltration using limma, ggpubr R packages, and tumor immune estimation resource 2 (TIMER2: <http://timer.cistrome.org/>) database between high and low risk groups of HNSCC patients. Then, we evaluated the correlation of risk score with immune cell infiltration in HNSCC patients using limma, scales, ggplot2, ggtext R packages, and the TIMER2 database. We explored the differences in immune function between HNSCC patients at high and low risk, by performing GSEA with GSEA 4.0.1 software, after downloading the gmt format files of IMMUNE_RESPONSE (M19817) and IMMUNE_SYSTEM_PROCESS (M13664) gene sets from molecular signatures' database (<http://www.gsea-msigdb.org/gsea/msigdb/search.jsp>).

Examining the relationship among RNA-binding proteins (RBPs), PHILTlncRNAs, PD-1 and PD-L1 in HNSCC

We analyzed the differential expression of *PDCD1* (gene encoding PD-1), *CD274* (gene encoding PD-L1) and two RBPs (*DNMT1* and *ZC3H12D*) in high and low risk groups using limma and ggpubr R packages. Correlation analysis of the expression of genes encoding PD-1 and PD-L1 and PHILTlncRNAs was conducted with ggplot2, ggpubr and ggExtra R packages. To investigate the effect of PD-1 or PD-L1 expression combined with PHILTlncRNAs on the survival of HNSCC patients, we performed Kaplan-Meier survival analysis using survivor and survminer R packages with log-rank tests. The correlation of DNMT1, ZC3H12D, PD-1 and PD-L1 expression were analyzed by “Correlation Analysis” with Pearson correlation coefficient using data from TCGA database in the GEPIA2 (Gene Expression Profiling Interactive Analysis 2: <http://gepia2.cancer-pku.cn/#degens>) platform. We also analyzed the correlation between *DNMT1* and *ZC3H12D* expression and CD4⁺ and CD8⁺ T cell infiltration, respectively, using the TIMER2 website “immune-gene” model, with partial Spearman's correlation. The relationship between PD-L1, DNMT1, PD-1 and ZC3H12D expression and clinical parameters of HNSCC patients was analyzed using the “immune-outcome” model. Finally, we evaluated promoter methylation differences between DNMT1 and ZC3H12D in HNSCC patients on the UALCAN database (<http://ualcan.path.uab.edu/analysis-prot.html>).

Mutation and Drug Sensitivity Analysis

We submitted the “Head and Neck Squamous Cell Carcinoma (TCGA, PanCancer Atlas)”, DNMT1, ZC3H12D, PD-1 (*PDCD1*) and PD-L1 (*CD274*) data to the “Query by gene” at the cBioPortal (<https://www.cbioportal.org/>) website. We obtained the mutation types and their frequency in these four genes in the “oncoprint” mode and genetic mutation differences in the altered and unaltered groups in the “plot” mode. Groupings and copy



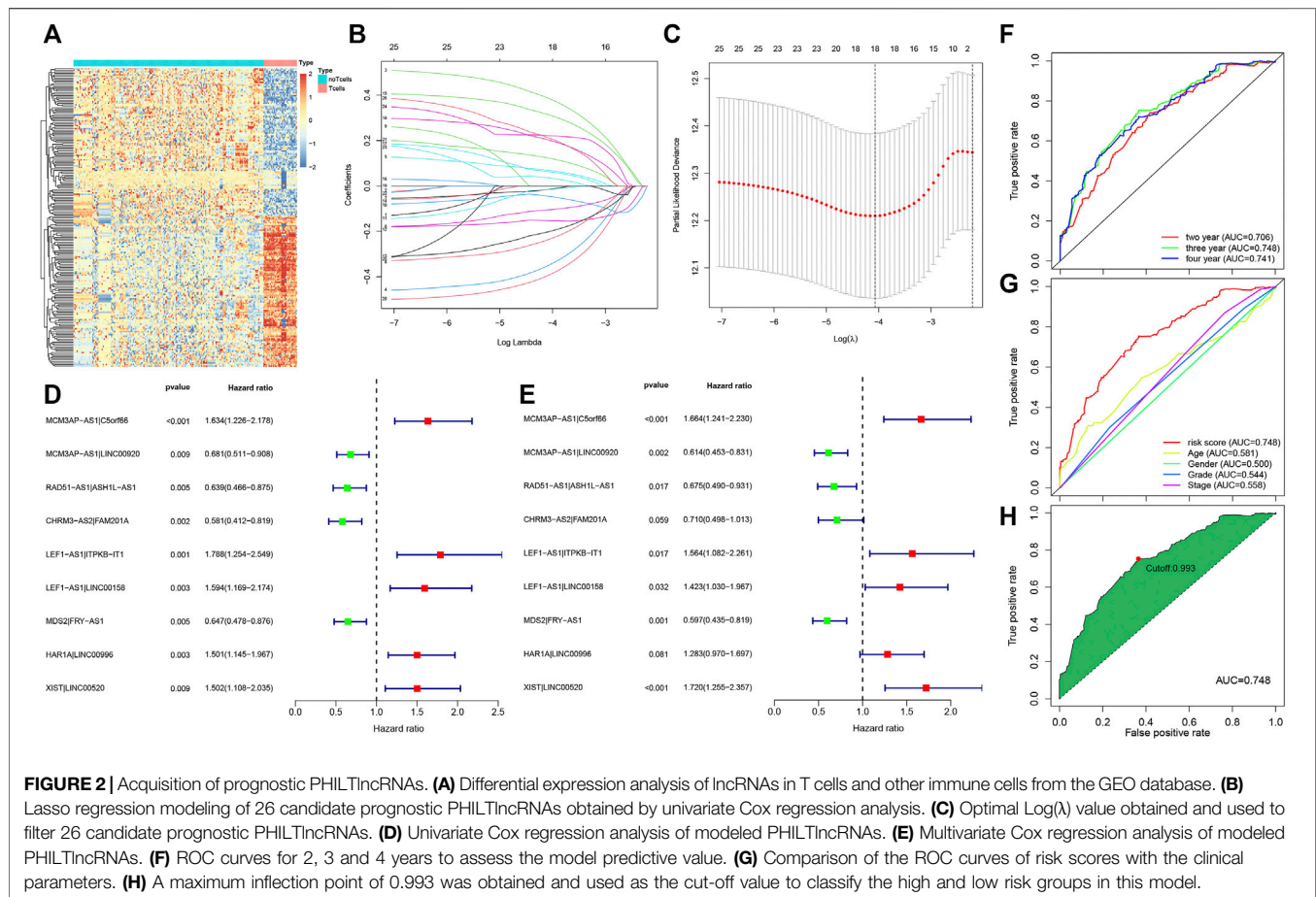
number variant type distributions were obtained in the “Comparison/Survival” modes. Finally, we performed drug sensitivity analysis using the limma, ggpubr, pRRophetic and ggplot2 R packages in HNSCC patients from TCGA database.

RESULTS

Acquisition of Prognostic PHILTincRNAs and Model Development

A flow chart illustrating the steps of the whole analysis was shown in **Figure 1**. Primary sites of the samples from the TCGA database were demonstrated in **Supplementary Table S1**. After differential expression analysis of lncRNAs between T cells and other immune cells from the GEO database (**Figure 2A**), we predicted 75 T-cell-specific lncRNAs ($|\log_{2}FC| > 1$, $FDR < 0.05$). Subsequently, the 75 T-cell-specific lncRNAs were intersected with lncRNAs of HNSCC and paired to obtain 848

PHILTincRNAs. Through univariate Cox regression analysis ($p < 0.01$), we obtained 26 candidate prognostic PHILTincRNAs, which were then screened by Lasso regression analysis for subsequent multivariate Cox regression analysis (**Figures 2B,C**). Ultimately, 9 prognostic PHILTincRNAs were identified and modeled by multivariate Cox regression analysis (**Figures 2D,E**). Then, the predictive survival value of the model was assessed by plotting the ROC curves for 2, 3, and 4 years with area under curve (AUC) values of 0.706, 0.748, and 0.741, respectively, indicating that the model was successfully developed (**Figure 2F**). In addition, the AUC value of the 3-years ROC curve was significantly higher than those of other clinical parameters, indicating that the model developed using the risk score was reliable in predicting survival (**Figure 2G**). Our subsequent calculation of the AIC value for each point on the 3-years ROC curve revealed that the cutoff value to divide high and low risk groups was the maximum inflection point of 0.993 (**Figure 2H**).



Evaluation of the Value of Prognostic PHILlncRNAs

The prognosis of HNSCC patients in the high risk group was poor ($p < 0.001$), as shown in **Figure 3A**. Further, as the risk score increased, the number of deaths in the HNSCC group of patients increased (**Figure 3B**). The grade ($p < 0.05$), T-stage ($p < 0.05$) and sex ($p < 0.001$) of HNSCC patients differed in the high and low risk groups, with females predominating in the high risk group (**Figure 3C**). As shown in **Figure 3D**, the risk score was higher in G2 than in G3 ($p = 0.021$) stage, higher in female patients than in male patients ($p = 7.3e-09$), lower in N0 than in N2 ($p = 0.024$) stage, higher in T3 than in T1 ($p = 0.018$) stage, higher in T3 than in T2 ($p = 0.035$) stage, higher in T4 than in T1 ($p = 0.006$) and T2 ($p = 0.0067$) stages. In the univariate Cox regression analysis, age (HR = 1.024, 95% CI (1.010–1.038), $p < 0.001$), stage (HR = 1.448, 95% CI (1.203–1.743), $p < 0.001$) and risk score (HR = 1.945, 95% CI (1.672–2.262), $p < 0.001$) were associated with the prognosis of HNSCC patients (**Figure 3E**). In the multivariate Cox regression analysis, age (HR = 1.023, 95% CI (1.008–1.038), $p = 0.002$), stage (HR = 1.422, 95% CI (1.176–1.718), $p < 0.001$) and risk score (HR = 1.869, 95% CI (1.582–2.209), $p < 0.001$) were associated with the prognosis of HNSCC patients (**Figure 3F**). We further stratified the HNSCC patients by

clinical parameters and performed multivariate Cox regression analysis for each stratum of HNSCC patients and included lncRNA-miRNA-mRNA in the analysis. The results were shown in **Supplementary Tables S2–S9**.

ceRNA Network of lncRNA-miRNA-mRNA in HNSCC-Infiltrating T Lymphocytes

We performed differential expression analysis on the mRNA data of HNSCC from the TCGA database ($|\log_{2}FC| > 2$, FDR < 0.05), and identified 1,543 differentially expressed mRNAs in HNSCC samples compared with normal samples (**Figure 4A**). We predicted 75 T-cell-specific lncRNAs that bind miRNAs using the miRcode database and identified 1,268 mRNAs that bind to these miRNAs using the miRDB, miRTarBase and TargetScan databases. We identified 34 hub mRNAs by intersecting the predicted mRNAs with the differentially expressed mRNAs in HNSCC patients (**Figure 4B**). The 34 hub mRNAs were used to screen the corresponding lncRNAs and miRNAs, and a ceRNA network was constructed using the cytoscape software to visually establish their interconnections (**Figure 4C**). The KEGG enrichment analysis performed on these 34 hub mRNAs showed that they were involved in the regulation of the rap1 signaling pathway, p53 signaling pathway and EGFR tyrosine

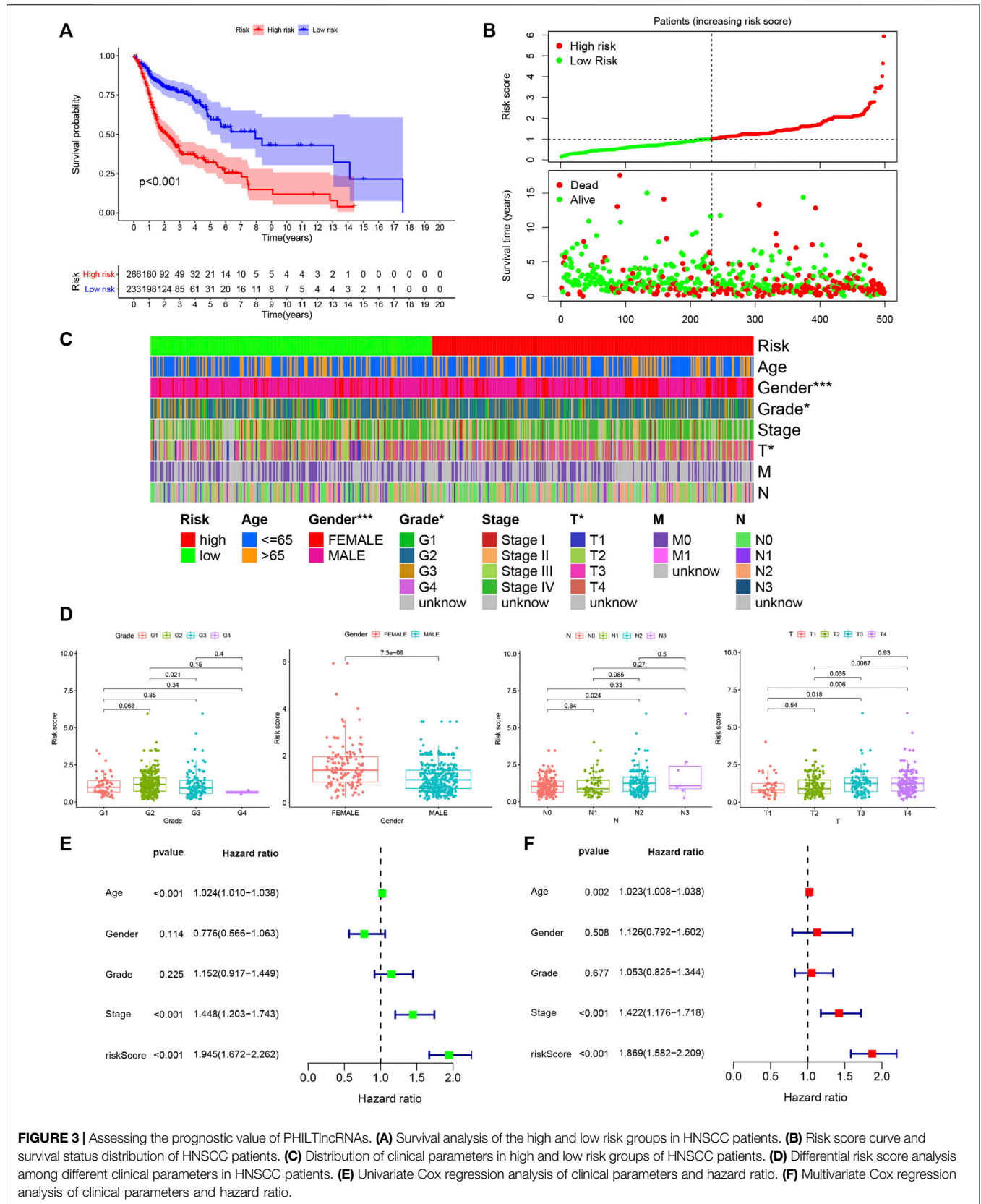
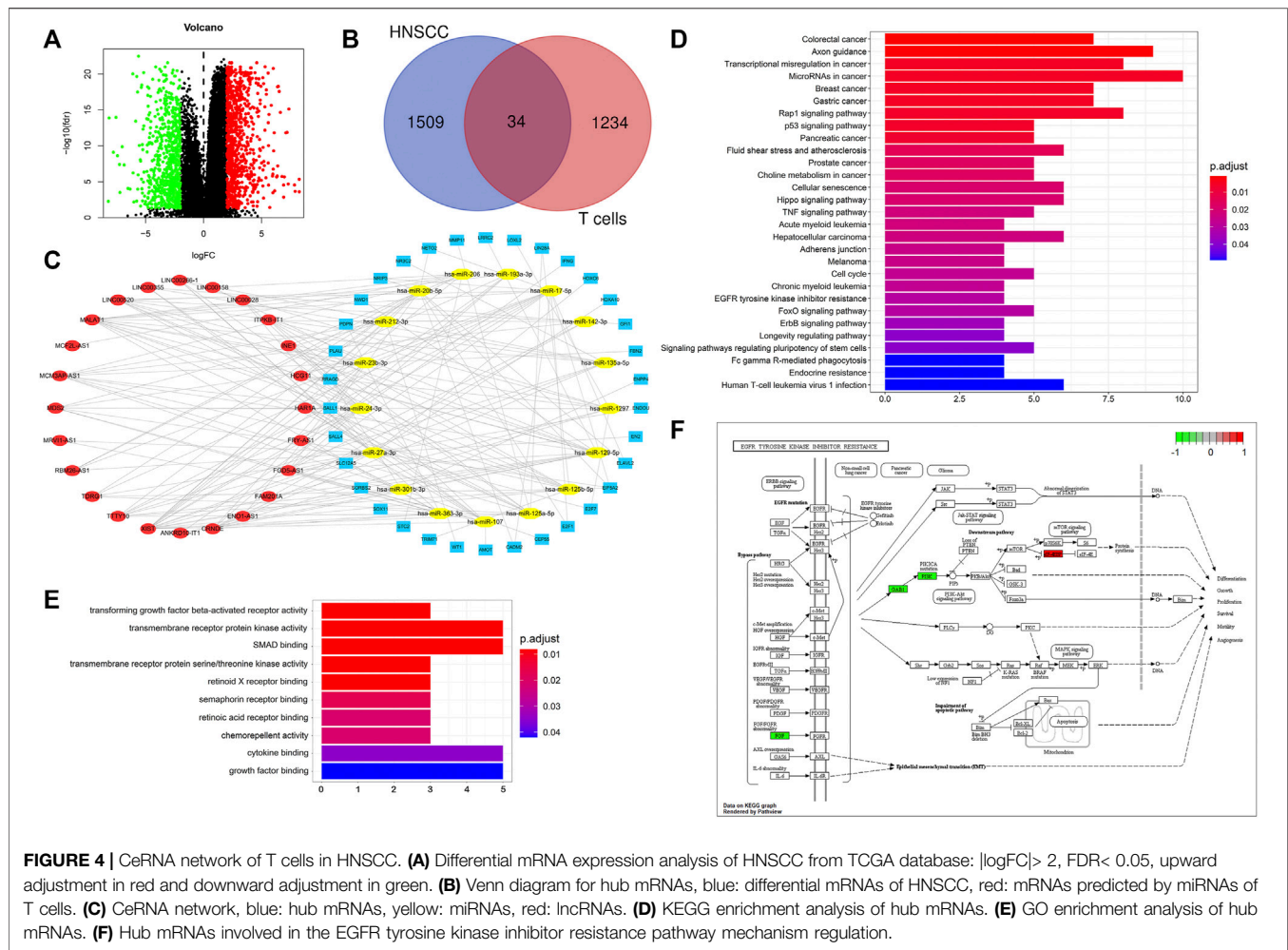


FIGURE 3 | Assessing the prognostic value of PHILlncRNAs. **(A)** Survival analysis of the high and low risk groups in HNSCC patients. **(B)** Risk score curve and survival status distribution of HNSCC patients. **(C)** Distribution of clinical parameters in high and low risk groups of HNSCC patients. **(D)** Differential risk score analysis among different clinical parameters in HNSCC patients. **(E)** Univariate Cox regression analysis of clinical parameters and hazard ratio. **(F)** Multivariate Cox regression analysis of clinical parameters and hazard ratio.



kinase inhibitor resistance, *etc* (Figure 4D). In addition, the GO enrichment analysis performed on these 34 hub mRNAs revealed that they were involved in various biological processes, including transforming growth factor beta-activated receptor activity, transmembrane receptor protein kinase activity and SMAD binding (Figure 4E). The hub mRNA was found to be involved in the mechanism of EGFR tyrosine kinase inhibitor resistance pathway, as shown in Figure 4F.

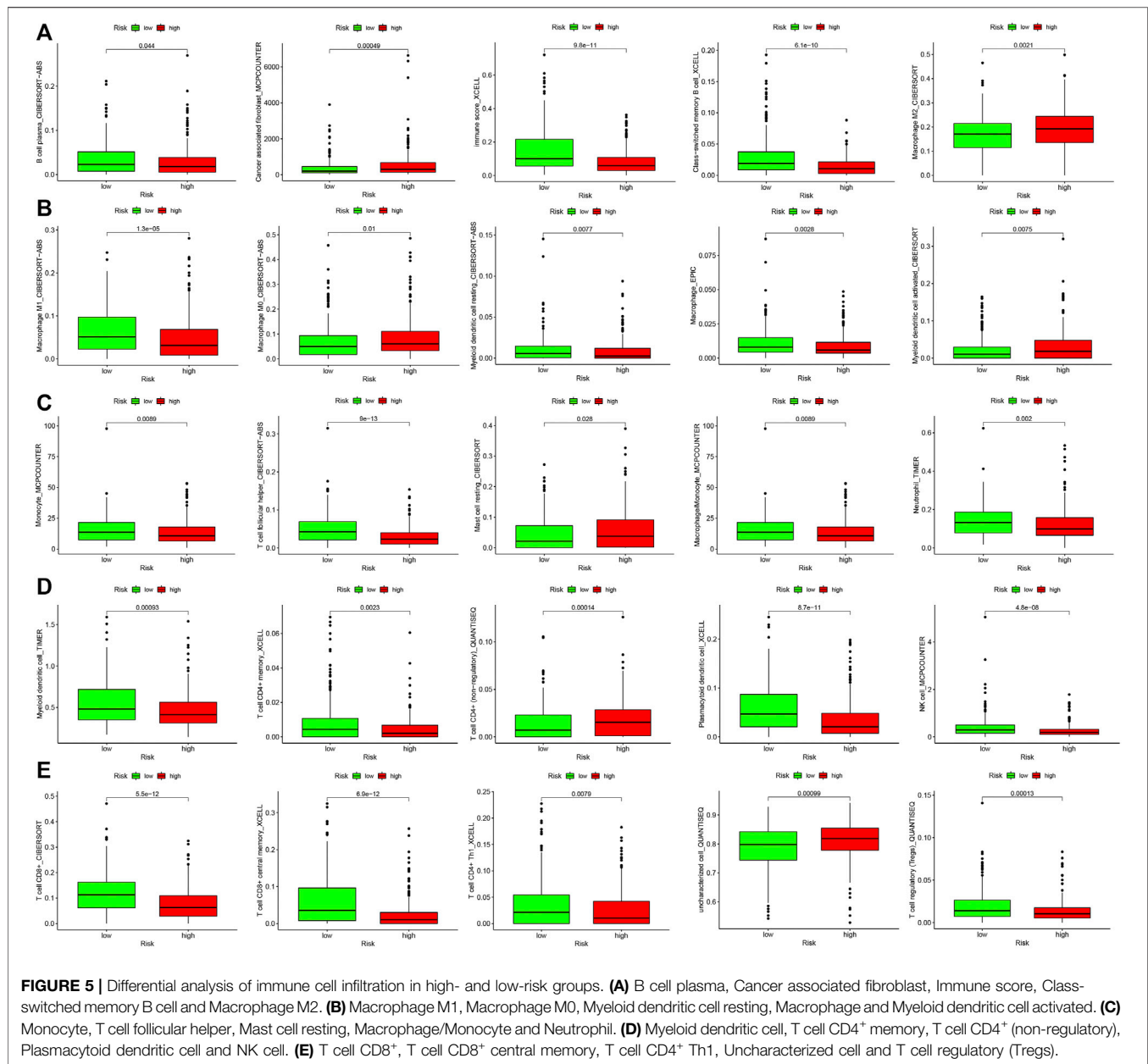
Analysis of Immune Cell Infiltration

The results of the differential analysis of immune cell infiltration in the high and low risk groups of HNSCC patients were shown in Figure 5, which showed that the extent of the immune cell infiltration decreased with increasing risk scores of HNSCC patients (Figure 6A). Our findings, by GSEA enrichment analysis, that the gene sets of IMMUNE_RESPONSE and IMMUNE_SYSTEM_PROCESS were both highly expressed in the low risk group and the gene sets in the low risk group were enriched in immune response ($NES = 2.05$, $FDR < 0.001$) and immune system process ($NES = 2.06$, $FDR = 0.01$) further verified the differences in immune function between the high and low risk groups, and also implied that the immune response and immune

system process were biologically active in the low risk group of HNSCC patients (Figure 6B).

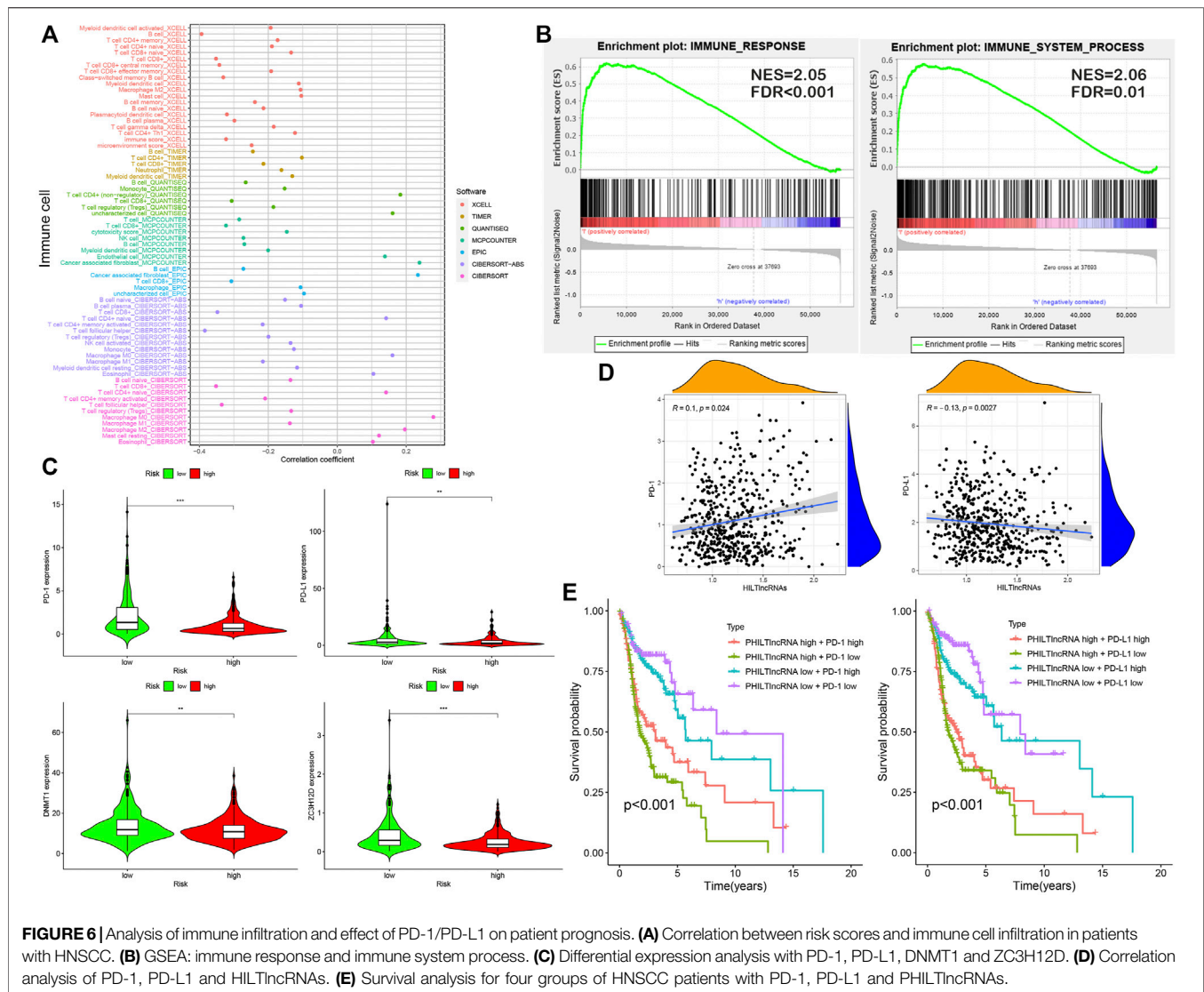
Examining the Relationship Among RBPs, PHILTlncRNAs, PD-1 and PD-L1 in HNSCC

PD-1 and PD-L1 are immunotherapeutic targets commonly used in clinical practice; While RBPs, DNMT1 and ZC3H12D, are closely associated with tumors progression (Gerstberger et al., 2014; Du et al., 2018; Jiang et al., 2019; Zhu et al., 2021). In this study, we found that the genes encoding PD-1 and PD-L1, DNMT1 and ZC3H12D were highly expressed in the low risk group of HNSCC patients (Figure 6C). In addition, the HILTlncRNAs were found to be positively correlated with the expression of the gene encoding PD-1 ($R = 0.1$ and $p = 0.024$), while HILTlncRNAs were found to be negatively correlated with the expression of the gene encoding PD-L1 ($R = -0.13$ and $p = 0.0027$) (Figure 6D). As shown in Figure 6E, we divided the HNSCC patients into four groups, and HNSCC patients in the low risk group based on PHILTlncRNAs and PD-1 low expression had the best prognosis compared with the other three groups, while the HNSCC patients in high risk group



and PD-1 low expression had the worst prognosis compared with the other three groups. The survival rate of HNSCC patients with high PD-1 expression in the low risk group was lower than that in the other groups, while high PD-1 expression in the high risk group was beneficial to improve the survival rate of HNSCC patients ($p < 0.001$). It was revealed similar effects as those of PHILTncRNAs and PD-L1 on the survival of HNSCC patients ($p < 0.001$). To investigate whether the two RBPs (DNMT1 and ZC3H12D) were related to PD-1 and PD-L1, we performed correlation analysis and found that DNMT1 ($p = 2.2e-16$ and $R = 0.35$) and ZC3H12D ($p < 0.001$ and $R = 0.72$) were positively correlated with the expression of the gene encoding PD-1. DNMT1 ($p = 0.0056$ and $R = 0.12$) and ZC3H12D ($p = 0.00023$ and $R = 0.16$)

were both positively correlated with the gene encoding PD-L1 (**Figure 7A**). DNMT1 was positively correlated with CD8⁺ T cell ($R = 0.295$, $p = 2.27e-11$ and MCPCOUNTER algorithm) and CD4⁺ Th2 cell ($R = 0.438$, $p = 1.94e-24$ and XCELL algorithm) infiltration. ZC3H12D was positively correlated with CD8⁺ T cell ($R = 0.65$, $p = 2.25e-60$ and MCPCOUNTER algorithm) and CD4⁺ memory cell ($R = 0.486$, $p = 1.40e-30$ and XCELL algorithm) infiltration (**Figure 7B**). We also found that the expression of both DNMT1 and gene encoding PD-1 in HNSCC HPV + patients was negatively correlated with clinical parameters (race, sex, purity, stage and age) ($p < 0.05$). The expression of ZC3H12D in HNSCC, HNSCC HPV+ and HNSCC HPV- patients ($p < 0.05$) was negatively correlated with clinical parameters (**Figure 7C**). We also found that the promoter methylation level of DNMT1 was differentially expressed in HNSCC



and normal samples, Grade 2 and Grade 4, and in stage 2, 3 and 4. Additionally, the promoter methylation level of ZC3H12D was differentially expressed in HNSCC and normal individuals, and in Grade 1 and Grade 2 (Figure 7D).

Mutation and Drug Sensitivity Analysis

The mutations in *DNMT1*, *ZC3H12D*, PD-1 (*PDCD1*) and PD-L1 (*CD274*) detected in HNSCC patients were shown in Figure 8A. We included *DNMT1*, *ZC3H12D*, PD-1 (*PDCD1*) and PD-L1 (*CD274*) into the mutation classification. HNSCC patients were divided into the mutated group as long as one gene in the patient was mutated. *ERMP1*, *PDCD1LG2*, *PLGRKT*, *KIAA 2026*, *RIC1*, *PTPRD* and *MLANA* ($p < 0.001$) were mutated at high frequency in the mutant group (Figure 8B). Subsequently, after further refining the grouping into the altered, PD-L1, DNMT1, PD-1, unaltered and ZC3H12D groups, we observed that one HNSCC patient had simultaneous mutations in the gene encoding PD-L1 and *ZC3H12D* (Figure 8C). Figure 8D showed DNMT1

mRNA expression and ZC3H12D mRNA expression among the copy number variant types of PD-1, PD-L1. Finally, we analyzed the response of HNSCC to chemotherapeutic agents. HNSCC patients in the low risk group were more sensitive to mitomycin C ($p = 0.0076$), JNK inhibitor VIII ($p = 0.0033$), AKT inhibitor VIII ($p = 0.0038$) and rapamycin ($p = 0.0079$), while less sensitive to epothilone B ($p = 0.0017$) and OSI 906 ($p = 0.00083$) compared with the patients in the high risk group, as can be concluded from the half maximal inhibitory concentration (IC_{50}) (Figure 8E).

DISCUSSION

The metastasis and recurrence of HNSCC may be attributed to the abnormal interaction of immune cells with tumor cells and stromal cells in the TME (Zhang et al., 2020). Infiltrating cells in HNSCC were often divided into two types, one promoted tumor growth and the other inhibited it. The abundant tumor-

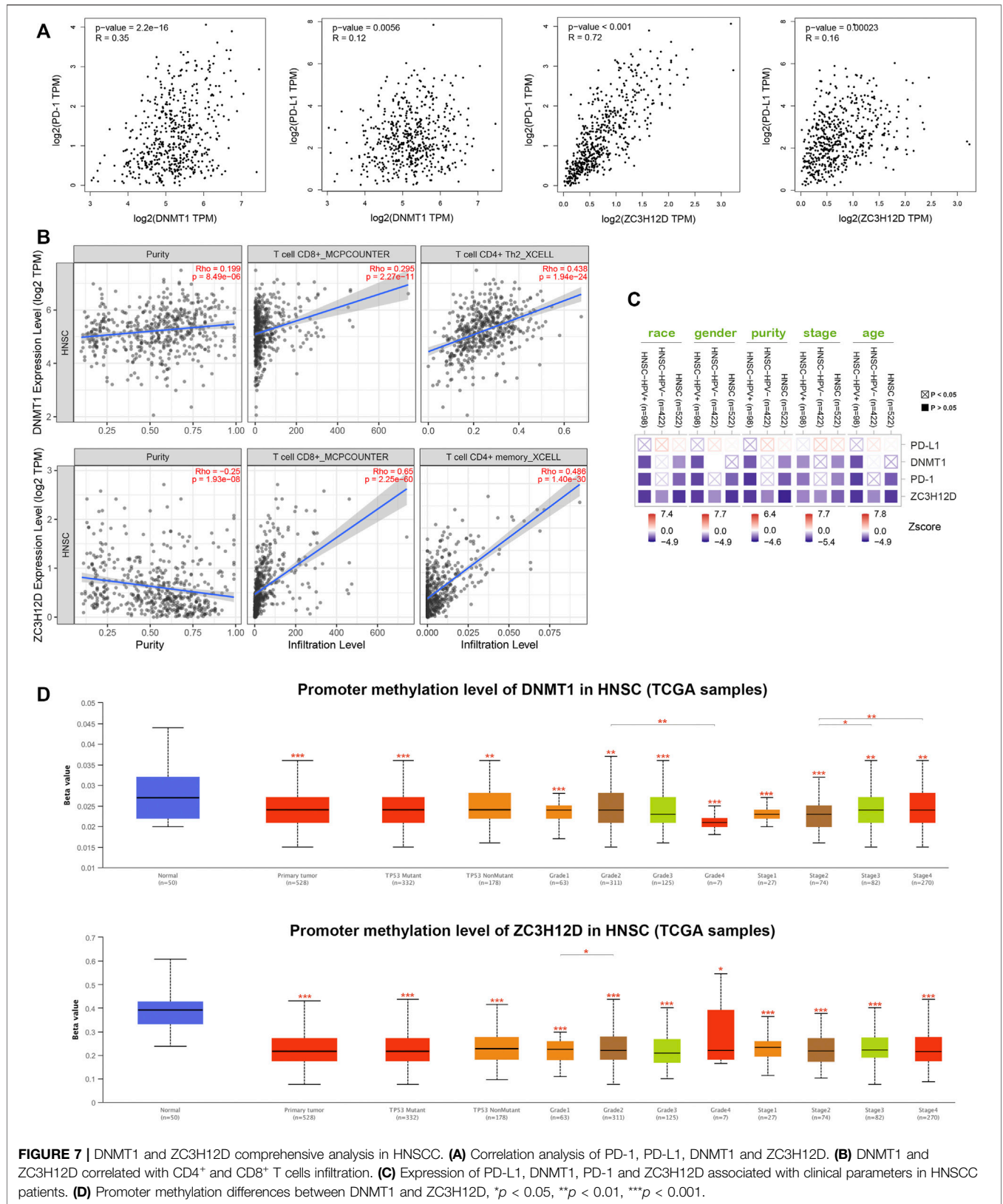


FIGURE 7 | DNMT1 and ZC3H12D comprehensive analysis in HNSCC. **(A)** Correlation analysis of PD-1, PD-L1, DNMT1 and ZC3H12D. **(B)** DNMT1 and ZC3H12D correlated with CD4⁺ and CD8⁺ T cells infiltration. **(C)** Expression of PD-L1, DNMT1, PD-1 and ZC3H12D associated with clinical parameters in HNSCC patients. **(D)** Promoter methylation differences between DNMT1 and ZC3H12D, *p < 0.05, **p < 0.01, ***p < 0.001.

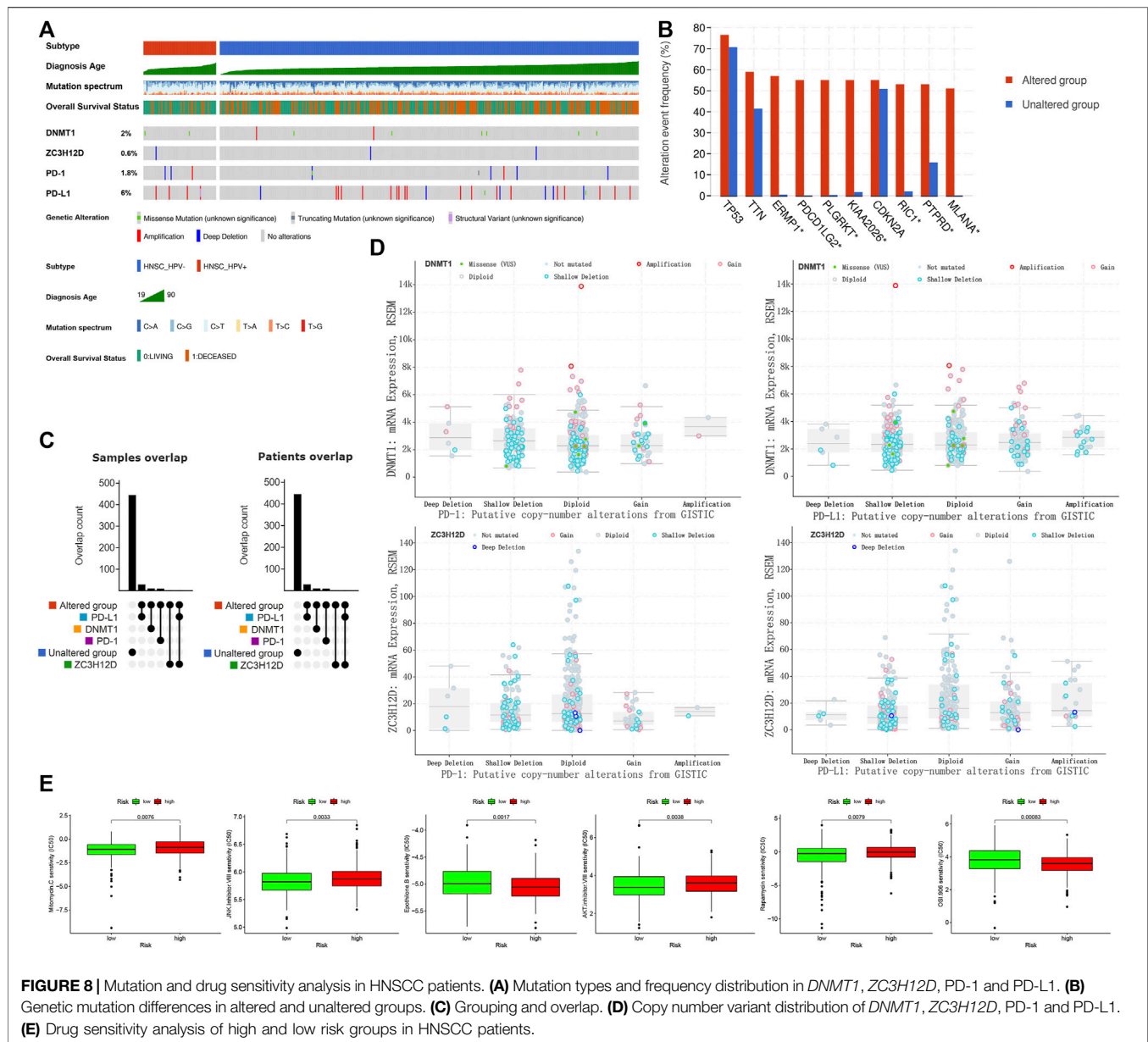


FIGURE 8 | Mutation and drug sensitivity analysis in HNSCC patients. **(A)** Mutation types and frequency distribution in *DNMT1*, *ZC3H12D*, PD-1 and PD-L1. **(B)** Genetic mutation differences in altered and unaltered groups. **(C)** Grouping and overlap. **(D)** Copy number variant distribution of *DNMT1*, *ZC3H12D*, PD-1 and PD-L1. **(E)** Drug sensitivity analysis of high and low risk groups in HNSCC patients.

associated macrophages (TAMs) infiltration in HNSCC was often accompanied by poor prognosis and lymphatic metastasis (Ni et al., 2015; Weber et al., 2016). Macrophages/monocytes in the TME regulated HNSCC stem cells through cluster of differentiation 44 (CD44) (Gomez et al., 2020). Serum IL-6, secreted by monocytes, was a predictor of relapse and survival in HNSCC patients (Kross et al., 2008). Exosomes secreted by HNSCC cells were aggregated in the TME and promoted endothelial cells to angiogenesis (Ludwig et al., 2018). Macrophages also secreted vascular endothelial growth factor (VEGF) to promote neovascularization (Sun et al., 2018). Significantly increased Tregs in the HNSCC TME was frequently accompanied by recurrence (Weed et al., 2013; Stasikowska-Kanicka et al., 2018). Myeloid-derived suppressor cells (MDSCs) reduced cysteine levels and produced arginine to

suppress T-lymphocyte activation (Parker et al., 2015), they also inhibited natural killer (NK) cell activity (Greene et al., 2020). Cancer-associated fibroblasts (CAFs) promoted T lymphocyte apoptosis, Tregs proliferation, and suppressed antitumor immunity in the TME (Takahashi et al., 2015). NK cells, CD8⁺ T cells, T helper 1 (Th1) cells, dendritic cells (DCs), M1 TAMs and N1 tumor-associated neutrophils (TANs) often played an antitumor role in the TME (Peltanova et al., 2019; Chen et al., 2020; Elmusrati et al., 2021). NK cells secreted immune interferon γ (IFN- γ), which induced infiltration of Th1 cells and MDSCs, and triggered adaptive immunity (Morvan and Lanier, 2016). NK cells recognized major histocompatibility complex class I (MHC-I) on the surface of tumor cells and secreted perforin and granzyme B to induce tumor cell death (Morvan and Lanier, 2016; Santos et al., 2019). TANs triggered CD8⁺ T lymphocyte

proliferation and cancer cell apoptosis (Moses and Brandau, 2016; Michaeli et al., 2017). Tumor-infiltrating CD8 T+ cells can either produce granzymes or perforin to directly kill tumor cells or produce IFN- γ and tumor necrosis factor (TNF) to mediate cytotoxic antitumor immune responses (Hadrup et al., 2013). However, the precise classification of infiltrating immune cells in HNSCC needs to be further explored. The biomarkers in the TME and infiltrating immune cell phenotype may change in the malignant progression of the tumor, and the staging of a HNSCC based on these changes need to be investigated. The molecular mechanisms underlying the invasive edge of HNSCC also need to be studied in depth. Although lncRNAs are not translated into proteins, they can regulate tumor biology by affecting miRNA and mRNAs. lncRNAs played an important role in the TME through transducing signaling (Botti et al., 2019). For instance, lncRNA CamK-A activated the CaMK-NF- κ B axis involved in TME remodeling (Sang et al., 2018). Besides, lncRNAs were involved in tumor-stroma crosstalk, and thus can be used as potential tumor biomarkers (Zhou et al., 2020).

Infiltrating T lymphocytes in the TME affected HNSCC progression. However, there were few studies focusing on lncRNA regulatory networks in HNSCC-infiltrating T lymphocytes. The role of lncRNAs in infiltrating T lymphocytes in the HNSCC TME remains to be elucidated. Multiple studies have also revealed that lncRNAs were associated with HNSCC patient prognosis. Chen *et al.* screened seven prognostic immune-related lncRNAs by univariate and multivariate Cox regression analysis, and classified HNSCC patients into high and low risk groups based on these lncRNAs. Low-risk HNSCC patients have a better prognosis, with large infiltrations of immune cells. In their study, a dataset of the identified immune-related genes was obtained from the ImmPort database and used to identify immune related lncRNAs through a co-expression strategy. Those lncRNAs were defined as immune related lncRNAs (cor >0.4) (Chen et al., 2021). In the current study, we optimized our method to screen tumor-infiltrating T lymphocytes specific lncRNAs. Candidate prognostic lncRNAs were screened by univariate Cox regression analysis, followed by Lasso regression screening, and ultimately by multivariate Cox regression analysis, which improved the reliability of the results. We also classified the HNSCC patients into high and low risk groups based on the cutoff values on ROC curves instead of using median values. Several studies identified immune-related lncRNA pairs that could well predict HNSCC patient prognosis (Mao et al., 2020; Yin et al., 2021). However, the role of specific lncRNAs in infiltrating T lymphocytes in HNSCC remains unclear. In the current study, we identified 9 prognostic PHILT lncRNAs and further studied their role in HNSCC. We found the expression of the two RBPs, DNMT1 and

ZC3H12D, were positive associated with PD-1, PD-L1 expression. In agreement with our results, Liu et al. verified that DNMT1 positively correlated with PD-L1 expression in hepatocellular carcinoma (Liu et al., 2017). Yan et al. found that overexpression of DNMT1 resulted in an increase of PD-L1 in small cell lung cancer (SCLC) cells (Yan et al., 2016). However, the relationship between ZC3H12D and PD-1/PD-L1 has not been reported and need further verification in the future.

In conclusion, this study systematically analyzed HILT lncRNAs and proposed HILT lncRNAs as novel biomarkers to provide a theoretical basis for the research in the TME of HNSCC and to provide new ideas for clinical diagnosis, immune-targeted therapy and drug discovery.

DATA AVAILABILITY STATEMENT

The original contributions presented in the study are included in the article. Further inquiries can be directed to the corresponding authors.

AUTHOR CONTRIBUTIONS

LW: Methodology, Data curation, Writing—Original draft preparation. GY: Data curation. GL: Validation, Data Curation, Writing—Reviewing, Editing and Funding acquisition. YP: Conceptualization, Supervision, Writing—Reviewing and Editing, Funding acquisition.

FUNDING

This work was supported by the National Natural Science Foundation of China (81872200, 31900558), the Natural Science Foundation of Hubei Province (2020CFB298), the Zhongnan Hospital of Wuhan University Science, Technology and Innovation Seed Fund (ZNPY2018090, ZNPY2019002) and the Fundamental Research Funds for the Central Universities (2042019kf0139).

SUPPLEMENTARY MATERIAL

The Supplementary Material for this article can be found online at: <https://www.frontiersin.org/articles/10.3389/fphar.2021.795205/full#supplementary-material>

REFERENCES

- Botti, G., Scognamiglio, G., Aquino, G., Liguori, G., and Cantile, M. (2019). lncRNA HOTAIR in Tumor Microenvironment: What Role? *Int. J. Mol. Sci.* 20 (9), 2279. doi:10.3390/ijms20092279
- Cao, W., Liu, J. N., Liu, Z., Wang, X., Han, Z. G., Ji, T., et al. (2017). A Three-lncRNA Signature Derived from the Atlas of ncRNA in Cancer (TANRIC Database Predicts the Survival of Patients with Head and Neck Squamous Cell Carcinoma. *Oral Oncol.* 65, 94–101. doi:10.1016/j.oraloncology.2016.12.017
- Chen, S. M. Y., Krinsky, A. L., Woolaver, R. A., Wang, X., Chen, Z., and Wang, J. H. (2020). Tumor Immune Microenvironment in Head and Neck Cancers. *Mol. Carcinog* 59 (7), 766–774. doi:10.1002/mc.23162
- Chen, Y., Luo, T. Q., Xu, S. S., Chen, C. Y., Sun, Y., Lin, L., et al. (2021). An Immune-Related Seven-lncRNA Signature for Head and Neck Squamous Cell Carcinoma. *Cancer Med.* 10 (7), 2268–2285. doi:10.1002/cam4.3756

- Di Martino, J. S., Mondal, C., and Bravo-Cordero, J. J. (2019). Textures of the Tumour Microenvironment. *Essays Biochem.* 63 (5), 619–629. doi:10.1042/EBC20190019
- Diao, P., Song, Y., Ge, H., Wu, Y., Li, J., Zhang, W., et al. (2019). Identification of 4-lncRNA Prognostic Signature in Head and Neck Squamous Cell Carcinoma. *J. Cel Biochem* 120 (6), 10010–10020. doi:10.1002/jcb.28284
- Du, W. W., Yang, W., Li, X., Awan, F. M., Yang, Z., Fang, L., et al. (2018). A Circular RNA Circ-DNMT1 Enhances Breast Cancer Progression by Activating Autophagy. *Oncogene* 37 (44), 5829–5842. doi:10.1038/s41388-018-0369-y
- Elmusrati, A., Wang, J., and Wang, C. Y. (2021). Tumor Microenvironment and Immune Evasion in Head and Neck Squamous Cell Carcinoma. *Int. J. Oral Sci.* 13 (1), 24. doi:10.1038/s41368-021-00131-7
- Gerstberger, S., Hafner, M., and Tuschl, T. (2014). A Census of Human RNA-Binding Proteins. *Nat. Rev. Genet.* 15 (12), 829–845. doi:10.1038/nrg3813
- Gomez, K. E., Wu, F., Keysar, S. B., Morton, J. J., Miller, B., Chimed, T. S., et al. (2020). Cancer Cell CD44 Mediates Macrophage/Monocyte-Driven Regulation of Head and Neck Cancer Stem Cells. *Cancer Res.* 80 (19), 4185–4198. doi:10.1158/0008-5472.CAN-20-1079
- Greene, S., Robbins, Y., Mydlarz, W. K., Huynh, A. P., Schmitt, N. C., Friedman, J., et al. (2020). Inhibition of MDSC Trafficking with SX-682, a CXCR1/2 Inhibitor, Enhances NK-Cell Immunotherapy in Head and Neck Cancer Models. *Clin. Cancer Res.* 26 (6), 1420–1431. doi:10.1158/1078-0432.CCR-19-2625
- Hadrup, S., Donia, M., and Thor Straten, P. (2013). Effector CD4 and CD8 T Cells and Their Role in the Tumor Microenvironment. *Cancer Microenviron* 6 (2), 123–133. doi:10.1007/s12307-012-0127-6
- Jiang, Y., Chen, M., Nie, H., and Yuan, Y. (2019). PD-1 and PD-L1 in Cancer Immunotherapy: Clinical Implications and Future Considerations. *Hum. Vaccin. Immunother.* 15 (5), 1111–1122. doi:10.1080/21645515.2019.1571892
- Johnson, D. E., Burtneess, B., Leemans, C. R., Lui, V. W. Y., Bauman, J. E., and Grandis, J. R. (2020). Head and Neck Squamous Cell Carcinoma. *Nat. Rev. Dis. Primers* 6 (1), 92. doi:10.1038/s41572-020-00224-3
- Kesselring, R., Thiel, A., Pries, R., Trenkle, T., and Wollenberg, B. (2010). Human Th17 Cells Can Be Induced through Head and Neck Cancer and Have a Functional Impact on HNSCC Development. *Br. J. Cancer* 103 (8), 1245–1254. doi:10.1038/sj.bjc.6605891
- Kross, K. W., Heimdal, J. H., Olsnes, C., Olofsson, J., and Aarstad, H. J. (2008). Co-culture of Head and Neck Squamous Cell Carcinoma Spheroids with Autologous Monocytes Predicts Prognosis. *Scand. J. Immunol.* 67 (4), 392–399. doi:10.1111/j.1365-3083.2008.02072.x
- Lei, Y., Xie, Y., Tan, Y. S., Prince, M. E., Moyer, J. S., Nör, J., et al. (2016). Telltale Tumor Infiltrating Lymphocytes (TIL) in Oral, Head & Neck Cancer. *Oral Oncol.* 61, 159–165. doi:10.1016/j.oraloncology.2016.08.003
- Liu, J., Liu, Y., Meng, L., Liu, K., and Ji, B. (2017). Targeting the PD-L1/dnmt1 axis in Acquired Resistance to Sorafenib in Human Hepatocellular Carcinoma. *Oncol. Rep.* 38 (2), 899–907. doi:10.3892/or.2017.5722
- Liu, J. F., Wu, L., Yang, L. L., Deng, W. W., Mao, L., Wu, H., et al. (2018). Blockade of TIM3 Relieves Immunosuppression through Reducing Regulatory T Cells in Head and Neck Cancer. *J. Exp. Clin. Cancer Res.* 37 (1), 44. doi:10.1186/s13046-018-0713-7
- Liu, Z., McMichael, E. L., Shayan, G., Li, J., Chen, K., Srivastava, R., et al. (2018). Novel Effector Phenotype of Tim-3+ Regulatory T Cells Leads to Enhanced Suppressive Function in Head and Neck Cancer Patients. *Clin. Cancer Res.* 24 (18), 4529–4538. doi:10.1158/1078-0432.CCR-17-1350
- Ludwig, N., Yerneni, S. S., Razzo, B. M., and Whiteside, T. L. (2018). Exosomes from HNSCC Promote Angiogenesis through Reprogramming of Endothelial Cells. *Mol. Cancer Res.* 16 (11), 1798–1808. doi:10.1158/1541-7786.MCR-18-0358
- Ma, H., Chang, H., Yang, W., Lu, Y., Hu, J., and Jin, S. (2020). A Novel IFN α -Induced Long Noncoding RNA Negatively Regulates Immunosuppression by Interrupting H3K27 Acetylation in Head and Neck Squamous Cell Carcinoma. *Mol. Cancer* 19 (1), 4. doi:10.1186/s12943-019-1123-y
- Mao, R., Chen, Y., Xiong, L., Liu, Y., and Zhang, T. (2020). Identification of a Nomogram Based on an 8-lncRNA Signature as a Novel Diagnostic Biomarker for Head and Neck Squamous Cell Carcinoma. *Aging (Albany NY)* 12 (20), 20778–20800. doi:10.18632/aging.104014
- McDermott, J. D., and Bowles, D. W. (2019). Epidemiology of Head and Neck Squamous Cell Carcinomas: Impact on Staging and Prevention Strategies. *Curr. Treat. Options. Oncol.* 20 (5), 43. doi:10.1007/s11864-019-0650-5
- Michaeli, J., Shaul, M. E., Mishalian, I., Hovav, A. H., Levy, L., Zolotriov, L., et al. (2017). Tumor-associated Neutrophils Induce Apoptosis of Non-activated CD8 T-Cells in a TNF α and NO-dependent Mechanism, Promoting a Tumor-Supportive Environment. *Oncoimmunology* 6 (11), e1356965. doi:10.1080/2162402X.2017.1356965
- Morvan, M. G., and Lanier, L. L. (2016). NK Cells and Cancer: You Can Teach Innate Cells New Tricks. *Nat. Rev. Cancer* 16 (1), 7–19. doi:10.1038/nrc.2015.5
- Moses, K., and Brandau, S. (2016). Human Neutrophils: Their Role in Cancer and Relation to Myeloid-Derived Suppressor Cells. *Semin. Immunol.* 28 (2), 187–196. doi:10.1016/j.smim.2016.03.018
- Nguyen, N., Bellile, E., Thomas, D., McHugh, J., Rozek, L., Virani, S., et al. (2016). Tumor Infiltrating Lymphocytes and Survival in Patients with Head and Neck Squamous Cell Carcinoma. *Head Neck* 38 (7), 1074–1084. doi:10.1002/hed.24406
- Ni, Y. H., Ding, L., Huang, X. F., Dong, Y. C., Hu, Q. G., and Hou, Y. Y. (2015). Microlocalization of CD68+ Tumor-Associated Macrophages in Tumor Stroma Correlated with Poor Clinical Outcomes in Oral Squamous Cell Carcinoma Patients. *Tumour Biol.* 36 (7), 5291–5298. doi:10.1007/s13277-015-3189-5
- Parker, K. H., Beury, D. W., and Ostrand-Rosenberg, S. (2015). Myeloid-Derived Suppressor Cells: Critical Cells Driving Immune Suppression in the Tumor Microenvironment. *Adv. Cancer Res.* 128, 95–139. doi:10.1016/bs.acr.2015.04.002
- Peltanova, B., Raudenska, M., and Masarik, M. (2019). Effect of Tumor Microenvironment on Pathogenesis of the Head and Neck Squamous Cell Carcinoma: a Systematic Review. *Mol. Cancer* 18 (1), 63. doi:10.1186/s12943-019-0983-5
- Sang, L. J., Ju, H. Q., Liu, G. P., Tian, T., Ma, G. L., Lu, Y. X., et al. (2018). lncRNA CamK-A Regulates Ca²⁺-Signaling-Mediated Tumor Microenvironment Remodeling. *Mol. Cel* 72 (1), 601–683. doi:10.1016/j.molcel.2018.10.024
- Santos, E. M., Rodrigues de Matos, F., Freitas de Moraes, E., Galvão, H. C., and de Almeida Freitas, R. (2019). Evaluation of Cd8+ and Natural Killer Cells Defense in Oral and Oropharyngeal Squamous Cell Carcinoma. *J. Craniomaxillofac. Surg.* 47 (4), 676–681. doi:10.1016/j.jcms.2019.01.036
- Stasikowska-Kanicka, O., Wągrowka-Danilewicz, M., and Danilewicz, M. (2018). Immunohistochemical Analysis of Foxp3+, CD4+, CD8+ Cell Infiltrates and PD-L1 in Oral Squamous Cell Carcinoma. *Pathol. Oncol. Res.* 24 (3), 497–505. doi:10.1007/s12253-017-0270-y
- Sun, H., Miao, C., Liu, W., Qiao, X., Yang, W., Li, L., et al. (2018). TGF- β 1/T β RII/Smad3 Signaling Pathway Promotes VEGF Expression in Oral Squamous Cell Carcinoma Tumor-Associated Macrophages. *Biophys. Res. Commun.* 497 (2), 583–590. doi:10.1016/j.bbrc.2018.02.104
- Sung, H., Ferlay, J., Siegel, R. L., Laversanne, M., Soerjomataram, I., Jemal, A., et al. (2021). Global Cancer Statistics 2020: GLOBOCAN Estimates of Incidence and Mortality Worldwide for 36 Cancers in 185 Countries. *CA A. Cancer J. Clin.* 71 (3), 209–249. doi:10.3322/caac.21660
- Takahashi, H., Sakakura, K., Kawabata-Iwakawa, R., Rokudai, S., Toyoda, M., Nishiyama, M., et al. (2015). Immunosuppressive Activity of Cancer-Associated Fibroblasts in Head and Neck Squamous Cell Carcinoma. *Cancer Immunol. Immunother.* 64 (11), 1407–1417. doi:10.1007/s00262-015-1742-0
- Wang, P., Jin, M., Sun, C. H., Yang, L., Li, Y. S., Wang, X., et al. (2018). A Three-lncRNA Expression Signature Predicts Survival in Head and Neck Squamous Cell Carcinoma (HNSCC). *Biosci. Rep.* 38 (6). doi:10.1042/BSR20181528
- Wang, R., Ma, Z., Feng, L., Yang, Y., Tan, C., Shi, Q., et al. (2018). lncRNA MIR31HG Targets HIF1A and P21 to Facilitate Head and Neck Cancer Cell Proliferation and Tumorigenesis by Promoting Cell-Cycle Progression. *Mol. Cancer* 17 (1), 162. doi:10.1186/s12943-018-0916-8
- Weber, M., Iliopoulos, C., Moebius, P., Büttner-Herold, M., Amann, K., Ries, J., et al. (2016). Prognostic Significance of Macrophage Polarization in Early Stage Oral Squamous Cell Carcinomas. *Oral Oncol.* 52, 75–84. doi:10.1016/j.oraloncology.2015.11.001
- Weed, D. T., Walker, G., De La Fuente, A. C., Nazarian, R., Vella, J. L., Gomez-Fernandez, C. R., et al. (2013). FOXP3 Subcellular Localization Predicts Recurrence in Oral Squamous Cell Carcinoma. *PLoS one* 8 (8), e71908. doi:10.1371/journal.pone.0071908
- Wu, L., Mao, L., Liu, J. F., Chen, L., Yu, G. T., Yang, L. L., et al. (2019). Blockade of TIGIT/CD155 Signaling Reverses T-Cell Exhaustion and Enhances Antitumor

- Capability in Head and Neck Squamous Cell Carcinoma. *Cancer Immunol. Res.* 7 (10), 1700–1713. doi:10.1158/2326-6066.CIR-18-0725
- Xue, K., Li, J., Nan, S., Zhao, X., and Xu, C. (2019). Downregulation of LINC00460 Decreases STC2 and Promotes Autophagy of Head and Neck Squamous Cell Carcinoma by Up-Regulating microRNA-206. *Life Sci.* 231, 116459. doi:10.1016/j.lfs.2019.05.015
- Yan, F., Pang, J., Peng, Y., Molina, J. R., Yang, P., and Liu, S. (2016). Elevated Cellular PD1/PD-L1 Expression Confers Acquired Resistance to Cisplatin in Small Cell Lung Cancer Cells. *PLoS one* 11 (9), e0162925. doi:10.1371/journal.pone.0162925
- Yin, J., Li, X., Lv, C., He, X., Luo, X., Li, S., et al. (2021). Immune-Related lncRNA Signature for Predicting the Immune Landscape of Head and Neck Squamous Cell Carcinoma. *Front. Mol. Biosci.* 8, 689224. doi:10.3389/fmolb.2021.689224
- Zhang, B., Wang, H., Guo, Z., and Zhang, X. (2019). Prediction of Head and Neck Squamous Cell Carcinoma Survival Based on the Expression of 15 lncRNAs. *J. Cel Physiol* 234 (10), 18781–18791. doi:10.1002/jcp.28517
- Zhang, X., Shi, M., Chen, T., and Zhang, B. (2020). Characterization of the Immune Cell Infiltration Landscape in Head and Neck Squamous Cell Carcinoma to Aid Immunotherapy. *Mol. Ther. Nucleic Acids* 22, 298–309. doi:10.1016/j.omtn.2020.08.030
- Zhou, L., Zhu, Y., Sun, D., and Zhang, Q. (2020). Emerging Roles of Long Non-coding RNAs in the Tumor Microenvironment. *Int. J. Biol. Sci.* 16 (12), 2094–2103. doi:10.7150/ijbs.44420
- Zhu, M., Wu, Y., Wang, Z., Lin, M., Su, B., Li, C., et al. (2021). miR-128-3p Serves as an Oncogenic microRNA in Osteosarcoma Cells by Downregulating ZC3H12D. *Oncol. Lett.* 21 (2), 152. doi:10.3892/ol.2020.12413

Conflict of Interest: The authors declare that the research was conducted in the absence of any commercial or financial relationships that could be construed as a potential conflict of interest.

Publisher's Note: All claims expressed in this article are solely those of the authors and do not necessarily represent those of their affiliated organizations, or those of the publisher, the editors and the reviewers. Any product that may be evaluated in this article, or claim that may be made by its manufacturer, is not guaranteed or endorsed by the publisher.

Copyright © 2022 Wang, Yang, Liu and Pan. This is an open-access article distributed under the terms of the Creative Commons Attribution License (CC BY). The use, distribution or reproduction in other forums is permitted, provided the original author(s) and the copyright owner(s) are credited and that the original publication in this journal is cited, in accordance with accepted academic practice. No use, distribution or reproduction is permitted which does not comply with these terms.